Quenching of magnetic form factors of *s-d* shell nuclei ^{17}O, ^{25}Mg, ^{27}Al, ^{29}Si, and ^{31}P within the relativistic mean field model

Zaijun Wang,[1,*] Zhongzhou Ren,[2,3] Tiekuang Dong,[4] and Xiaoyong Guo[5]
[1]*School of Science, Tianjin University of Technology and Education, Tianjin 300222, China*
[2]*Department of Physics, Nanjing University, Nanjing 210008, China*
[3]*Center of Theoretical Nuclear Physics, National Laboratory of Heavy-Ion Accelerator at Lanzhou, Lanzhou 730000, China*
[4]*Purple Mountain Observatory, Chinese Academy of Sciences, Nanjing 210008, China*
[5]*School of Science, Tianjin University of Science and Technology, Tianjin 300457, China*
(Received 19 February 2015; revised manuscript received 22 May 2015; published 14 July 2015)

The magnetic form factors of the odd-A *s-d* shell nuclei ^{17}O, ^{25}Mg, ^{27}Al, ^{29}Si, and ^{31}P are studied within the relativistic frame with single-nucleon wave functions generated using the relativistic mean field model. Single valence-nucleon contributions to the nuclear magnetic form factors are calculated, and two sets of quenching ratios of the nuclear magnetic form factors relative to the single valence-nucleon contributions are extracted for each nucleus. It is found that the single valence-nucleon contributions can generally give a good approximate description for the shapes of the nuclear magnetic form factors, including the positions of the minima and maxima, and after the quenching ratios are applied the experimental data can be very well reproduced. The quenching ratios are compared with those obtained within some other nuclear models, and the physical implications for each nucleus are discussed. Calculations also show that no reasonable quenching ratios could be found for ^{27}Al when $\mu_{\text{expt.}}/\mu_{s.n.}$ is chosen as the $M1$ multipole quenching ratio. This implies that the common way of choosing $\mu_{\text{expt.}}/\mu_{s.n.}$ as the $M1$ multipole quenching ratio for the odd-A nuclei is not always valid.

DOI: 10.1103/PhysRevC.92.014309 PACS number(s): 21.10.Pc, 21.60.Cs, 25.30.Bf

I. INTRODUCTION

Elastic magnetic electron scattering provides a sensitive and direct way to study the magnetic properties and outermost-shell single-nucleon orbital shapes of nuclei. By explaining the experimental data with electron scattering theories and nuclear structure models, we can determine some important magnetic properties of nuclei, such as the current transition densities, the magnetic moments, the root-mean-square (rms) radii of the valence orbitals, and the quenching or spectroscopy ratios of the magnetic form factors, etc. Many researchers have made contributions in this field, and there have been a lot of significant and instructive calculations and discussions about nuclear magnetic form factors and relevant topics [1–29]. However, much of the earlier research is based on nonrelativistic nuclear structure models, which usually contain free parameters for specific nuclei, such as the harmonic oscillator potential model and the Woods-Saxon potential model plus the spin-orbit interaction. These models have played a very important and foundational role in the development of nuclear structure theories. The calculations of nuclear magnetic form factors based on these models have provided much useful information and greatly promoted further studies. Along with the development of studies of nuclear physics, a relativistic nuclear model, now known as the relativistic mean field (RMF) model or approximation, was put forward in the 1970s [30,31]. This model treats the atomic nucleus as a relativistic system based on meson exchange nucleon-nucleon interactions [30–34], and has been well developed, extensively studied, and widely used over the past years. It has been shown to be one of the most successful nuclear structure models in describing nuclear properties. For one thing, a lot of calculations [30–41] have shown that the RMF model can reproduce with good precision the binding energies, the separation energies, the rms radii of charge density distributions, and the single-nucleon wave functions. For another, unlike the harmonic oscillator potential model and the Woods-Saxon potential model, the relativistic mean field model has no free parameters for specific nuclei. In addition, some other calculations—such as the calculations of quasielastic electron scattering in the plane wave impulse approximation with relativistic effects contained [42], and in the relativistic plane wave impulse approximation and relativistic distorted wave impulse approximation [43–46] that uses wave functions from a relativistic mean field—have also shown that the relativistic mean field approximation can very well describe the shape of single-nucleon orbitals. Therefore, it would be interesting to calculate the magnetic form factors of nuclei within this relativistic nuclear model. The calculations could be a good complement to the results now available, obtained by predecessors within the other nuclear models, and provide more useful references for further and more involved studies.

In the present paper, we would like to calculate and discuss the magnetic form factors of the *s-d* shell nuclei ^{17}O, ^{25}Mg, ^{27}Al, ^{29}Si, and ^{31}P within the relativistic mean field model. The nucleus ^{17}O has a single neutron outside the doubly closed p shell; ^{25}Mg and ^{27}Al, with the *s-d* shell nearly half filled, have an odd number of neutrons and protons in the $1d_{5/2}$ orbital, respectively; ^{29}Si and ^{31}P, with the *s-d* shell also nearly half filled, have a single neutron and a single proton in the $2s_{1/2}$ subshell, respectively; so they are the prime examples of the odd-A nuclei in the *s-d* shell. Therefore, in

*zjwang@tute.edu.cn

view of the single-particle shell model, the magnetic form factors of these nuclei can be calculated with the single valence-nucleon wave functions, and the results would be typical and representative. Furthermore, the experimental data of these nuclei are available within a broad momentum transfer range. Then the calculated results can be compared with the experimental data, and the quenching ratios of the nuclear magnetic form factors relative to the single valence-nucleon contributions can be extracted and discussed and compared with the results obtained within some other nuclear models.

The paper is organized as follows. Section II gives the formalism of nuclear magnetic form factors in the relativistic frame. Section III is devoted to the numerical results and discussions. A summary is given in Sec. IV.

II. FORMALISM

In the relativistic frame, the single-particle wave functions [32,47] can be expressed as

$$\psi_{n\kappa m} = \begin{bmatrix} i\,[G(r)/r]\,\Phi_{\kappa m}(\hat{r}) \\ -[F(r)/r]\,\Phi_{-\kappa m}(\hat{r}) \end{bmatrix} = \begin{bmatrix} i|n\kappa m\rangle \\ -\overline{|n\kappa m\rangle} \end{bmatrix} = \begin{bmatrix} i\left|nl\tfrac{1}{2}jm\right\rangle \\ -\left|nl'\tfrac{1}{2}jm\right\rangle \end{bmatrix}, \tag{1}$$

where the total angular momentum quantum number j, the orbital angular momentum quantum numbers l, l', and the angular quantum number κ satisfy

$$j = |\kappa| - \frac{1}{2}, \tag{2}$$

$$\begin{aligned} l &= \kappa, & l' &= l-1 \quad (\kappa > 0), \\ l &= -(\kappa+1), & l' &= l+1 \quad (\kappa < 0), \end{aligned} \tag{3}$$

and the functions $\Phi_{\kappa m}$ in Eq. (1) are the spinor spherical harmonics, which are given by

$$\Phi_{\kappa m} = \sum_{m_l m_s} \left\langle l m_l \tfrac{1}{2} m_s \middle| l \tfrac{1}{2} jm \right\rangle Y_{lm_l} \chi_{m_s}. \tag{4}$$

In the single-particle shell model, only the unpaired valence nucleon contributes to the nuclear magnetic form factors. With the magnetic multipole operator $\hat{T}^{\rm mag}_{LM}(q)$, the contribution of the single valence nucleon to the Lth multipole of the nuclear magnetic form factors can be written as

$$F_{ML}(q) = \sqrt{\frac{4\pi}{2J_i+1}} \langle J_f \| \hat{T}^{\rm mag}_{L}(q) \| J_i \rangle, \tag{5}$$

where the multipole operator $\hat{T}^{\rm mag}_{LM}(q)$ [1,48,49] is defined by

$$\hat{T}^{\rm mag}_{LM}(q) = \int j_L(qr) \boldsymbol{Y}^{M}_{LL}(\hat{r}) \cdot \hat{\boldsymbol{J}}(\boldsymbol{r}) d^3\boldsymbol{r}, \tag{6}$$

and $\langle J_f \| \hat{T}^{\rm mag}_{L}(q) \| J_i \rangle$ in Eq. (5) is the reduced matrix element of $\hat{T}^{\rm mag}_{LM}(q)$, where q is the momentum transfer, and $\boldsymbol{Y}^{M}_{LL}(\hat{r})$ are the vector spherical harmonics [50].

With the formulas given in Refs. [32,51,52], the reduced matrix element $\langle J_f \| \hat{T}^{\rm mag}_{L}(q) \| J_i \rangle$ can be further expressed as

$$\langle J_f \| \hat{T}^{\rm mag}_{L}(q) \| J_i \rangle = -(q/2M_n) \langle n\kappa \| \lambda' \Sigma'^{M}_{L} \| n\kappa \rangle + (q/2M_n) \overline{\langle n\kappa \|} \lambda' \Sigma'^{M}_{L} \overline{\| n\kappa \rangle} + 2 \overline{\langle n\kappa \|} Q \Sigma^{M}_{L} \| n,\kappa \rangle. \tag{7}$$

In Eq. (7), the Q, M_n, and λ' are the electric charge, mass, and anomalous magnetic moment of the valence nucleon, respectively, and the operators Σ^{M}_{L} and Σ'^{M}_{L} [32,51,52] are given by

$$\Sigma^{M}_{L}(\boldsymbol{r}) \equiv \boldsymbol{M}^{M}_{LL}(\boldsymbol{r}) \cdot \boldsymbol{\sigma}, \quad \Sigma'^{M}_{L}(\boldsymbol{r}) \equiv -i\left[\nabla \times \boldsymbol{M}^{M}_{LL}(\boldsymbol{r})\right] \cdot \boldsymbol{\sigma}/q, \quad \boldsymbol{M}^{M}_{LL}(\boldsymbol{r}) \equiv j_L(qr) \boldsymbol{Y}^{M}_{LL}(\hat{r}).$$

The single-particle reduced matrix elements in Eq. (7) can be calculated with the formulas given by Edmonds [50], Willey [53], and Eq. (1). The integral expressions are as follows:

$$\begin{aligned} \langle n\kappa \| \Sigma'^{M}_{L} \| n\kappa \rangle = {} & \frac{(-1)^{l+1}}{q} \left(\frac{6}{4\pi}\right)^{1/2} (2l+1)(2j+1) \\ & \times \left[\begin{Bmatrix} l & l & L+1 \\ \frac{1}{2} & \frac{1}{2} & 1 \\ j & j & L \end{Bmatrix} \begin{pmatrix} l & L+1 & l \\ 0 & 0 & 0 \end{pmatrix} [L(2L+3)]^{1/2} \int dr\, r^2 j_L(qr) \left(\frac{d}{dr} + \frac{L+2}{r}\right) g^2(r) \right. \\ & \left. + \begin{Bmatrix} l & l & L-1 \\ \frac{1}{2} & \frac{1}{2} & 1 \\ j & j & L \end{Bmatrix} \begin{pmatrix} l & L-1 & l \\ 0 & 0 & 0 \end{pmatrix} [(L+1)(2L-1)]^{1/2} \int dr\, r^2 j_L(qr) \left(\frac{d}{dr} - \frac{L-1}{r}\right) g^2(r) \right], \end{aligned} \tag{8}$$

$$\overline{\langle n\kappa\|}\Sigma_L^{'M}\overline{\|n\kappa\rangle} = \frac{(-1)^{l'+1}}{q}\left(\frac{6}{4\pi}\right)^{1/2}(2l'+1)(2j+1)$$
$$\times\left[\begin{Bmatrix} l' & l' & L+1 \\ \frac{1}{2} & \frac{1}{2} & 1 \\ j & j & L \end{Bmatrix}\begin{pmatrix} l' & L+1 & l' \\ 0 & 0 & 0 \end{pmatrix}[L(2L+3)]^{1/2}\int dr\, r^2 j_L(qr)\left(\frac{d}{dr}+\frac{L+2}{r}\right)f^2(r)\right.$$
$$\left.+\begin{Bmatrix} l' & l' & L-1 \\ \frac{1}{2} & \frac{1}{2} & 1 \\ j & j & L \end{Bmatrix}\begin{pmatrix} l' & L-1 & l' \\ 0 & 0 & 0 \end{pmatrix}[(L+1)(2L-1)]^{1/2}\int dr\, r^2 j_L(qr)\left(\frac{d}{dr}-\frac{L-1}{r}\right)f^2(r)\right], \quad (9)$$

and

$$\overline{\langle n\kappa\|}\Sigma_L^{M}\|n\kappa\rangle = (-1)^{l'}\left(\frac{6}{4\pi}\right)^{1/2}(2L+1)(2j+1)[(2l+1)(2l'+1)]^{1/2}$$
$$\times\begin{Bmatrix} l' & l & L \\ \frac{1}{2} & \frac{1}{2} & 1 \\ j & j & L \end{Bmatrix}\begin{pmatrix} l' & L & l \\ 0 & 0 & 0 \end{pmatrix}\int dr\, r^2 j_L(qr)g(r)f(r), \quad (10)$$

where $g(r) = G(r)/r$, $f(r) = F(r)/r$ are the upper and lower components of the single-nucleon Dirac-4 spinors, and they are calculated using the relativistic mean field model with the NL-SH parameters [35] in the present research.

III. NUMERICAL RESULTS AND DISCUSSIONS

The nuclei ^{17}O, ^{25}Mg, ^{27}Al, ^{29}Si, and ^{31}P are typical odd-A s-d shell nuclei with an unpaired valence nucleon in the outermost shell, so the nuclear form factors of these nuclei can be calculated within the single-particle shell model. However, usually or most often, the nuclear form factors calculated within the single-particle shell model have deviations, large or small, from the experimental data because of many-body effects—such as those of the meson exchange and back-flow currents in the relativistic mean field—and core polarization effects. To include these effects in calculations and compare with experimental data, a commonly used method is to introduce the so-called quenching ratios or spectroscopy factors α_L to the scattering multipoles. In this way, the nuclear magnetic form factors can be expressed as

$$F_M^2(q) = \sum_{L=1}^{\text{odd}}\alpha_L^2 F_{ML}^2(q) f_{s.n.}^2(q) f_{c.o.m.}^2(q), \quad (11)$$

where the single-nucleon factor and center-of-mass factor in Eq. (11) are given by $f_{s.n.}(q) = [1 + (q/855\ \text{MeV})^2]^{-2}$ and $f_{c.o.m.}(q) = \exp(q^2b^2/4A)$, and $b = 1.0A^{1/6}$ fm is the oscillator length. Since the quenching ratios α_L are usually unknown, Eq. (11) is actually not commonly used to calculate the form factors directly, but to obtain the quenching ratios α_L within various different nuclear models. The quenching ratios then can be used to investigate to what extent the nuclear model(s) used can be applied to calculate the magnetic properties, to study the roles played by different multipoles in different momentum transfer regions, and to infer the contributions of the many-body and core polarization effects for a specific nucleus. In practice, the first quenching ratio is usually chosen to be the ratio of the experimental nuclear magnetic moment to the single-nucleon magnetic moment, $\mu_{\text{expt.}}/\mu_{s.n.}$, because of the limited amount of experimental data in the very low momentum transfer region, where the $M1$ component of the magnetic form factors dominates. The other quenching ratios are usually obtained along with the model parameters, such as the radius and surface diffuseness for the Woods-Saxon potential model and the oscillator length for the harmonic oscillator potential model, by fitting the theoretical form factors to the experimental data [7,15,18,19].

In the present paper, we use the relativistic mean field model to generate the single-nucleon wave functions, so there are no free model parameters to be fitted along with the quenching ratios for specific nuclei. In our calculations, we assume that the unpaired single nucleons in the ground states are in the $1d_{5/2}$ orbital for ^{17}O, ^{25}Mg, ^{27}Al and in the $2s_{1/2}$ orbital for ^{29}Si and ^{31}P. We calculate the single valence-nucleon contributions and then fit them to the experimental data with Eq. (11) in two cases: in one case, the quenching ratio α_1 is fixed to $\mu_{\text{expt.}}/\mu_{s.n.}$, as is the common practice, and the other quenching ratios are set to be free parameters; in another case, all the quenching ratios, including α_1, are set to be free parameters. Hence, two sets of quenching ratios are obtained for each nucleus.

The best fit quenching ratios obtained in the two cases are listed in Table I. In the table, the calculated rms radii for the corresponding valence-nucleon orbitals $[\langle r^2\rangle^{1/2}_{\text{valence}}$ (fm)] are also given for reference and comparison. In addition, the calculated charge distribution rms radii $[\langle r^2\rangle^{1/2}_{\text{charge}}$ (fm)] and the experimental charge distribution rms radii $[\langle r^2\rangle^{1/2}_{\text{expt.}}$ (fm)] [54] are also listed in the table. It is found from the table that the largest deviation of the calculated rms radius of charge distribution from the experimental data is less than 0.16 fm, which is the difference between the calculated result $\langle r^2\rangle^{1/2}_{\text{charge}} = 2.9614$ fm and the experimental value

TABLE I. The best fit quenching ratios for the magnetic form factors of ^{17}O, ^{25}Mg, ^{27}Al, ^{29}Si, and ^{31}P and the calculated rms radii for the valence-nucleon orbitals [$\langle r^2\rangle^{1/2}_{\text{valence}}$ (fm)] in the relativistic mean field model. Besides, the calculated charge distribution rms radii [$\langle r^2\rangle^{1/2}_{\text{charge}}$ (fm)] and the experimental charge distribution rms radii [54] [$\langle r^2\rangle^{1/2}_{\text{expt.}}$ (fm)] are also listed.

	^{17}O		^{25}Mg		^{27}Al		^{31}P		^{29}Si	
	α_1 fixed	α_1 free	α_1 fixed	α_1 free	α_1 fixed	α_1 free	α_1 fixed	α_1 free	α_1 fixed	α_1 free
α_1	0.990	0.887	0.447	0.333	1.304	0.716	0.405	0.526	0.290	0.532
α_3	0.475	0.514	0.124	0.205	1.90×10^{-4}	0.435				
α_5	0.880	0.891	0.499	0.510	0.575	0.606				
$\langle r^2\rangle^{1/2}_{\text{valence}}$ (fm)	3.405		3.276		3.284		3.851		3.817	
$\langle r^2\rangle^{1/2}_{\text{charge}}$ (fm)	2.7138		2.9614		2.9981		3.1674		3.0793	
$\langle r^2\rangle^{1/2}_{\text{expt.}}$ (fm) [54]	2.662		3.11(5) 3.003(11)		3.06(9) 3.05(5) 3.035(2)		3.19(3) 3.187(11) 3.187		3.13(5) 3.079(21)	

$\langle r^2\rangle^{1/2}_{\text{expt.}} = 3.11(5)$ fm for ^{25}Mg, and the corresponding relative deviation with respect to the experimental result is less than 4.94%. For the other calculated rms radii of charge distribution, the deviations from the experimental data are all less than 0.071 fm, which corresponds to a relative deviation of 2.31%. Therefore, for the considered nuclei, the rms radii of charge distribution are very well reproduced within the RMF model with the NL-SH parameters. In the following, we discuss the results of the magnetic form factors for the considered nuclei.

A. The nuclei ^{17}O, ^{25}Mg, and ^{27}Al

We obtained two sets of quenching ratios for the nucleus ^{17}O, as have been given in Table I: one set is $\alpha_1 = 0.887$, $\alpha_3 = 0.514$, and $\alpha_5 = 0.891$, and the other set is $\alpha_3 = 0.475$, $\alpha_5 = 0.880$ with α_1 fixed to $\mu_{\text{expt.}}/\mu_{s.n.} = 0.990$, where $\mu_{\text{expt.}} = -1.89379\mu_N$ [55] for ^{17}O and $\mu_{s.n.} = -1.9130\mu_N$ for the neutron. The values that we obtain for α_3 and α_5 agree with the results $\alpha_3 = 0.50 \pm 0.06$ and $\alpha_5 = 0.87 \pm 0.10$ obtained by Hicks [7] using the harmonic oscillator model plus corrections for exchange current effects, and are close to the values $\alpha_3 = 0.53 \pm 0.06$ and $\alpha_5 = 0.96 \pm 0.11$ obtained by the same author using the Woods-Saxon potential model with the meson exchange currents effects considered. In Table I, we also give the calculated rms radius for the $1d_{5/2}$ neutron orbital: the value is 3.405 fm, which is slightly larger than the result 3.36 fm obtained by fitting to the experimental data using the Woods-Saxon potential model by Kalantar-Nayestanaki [17] and a little smaller than the result (3.56 ± 0.09) fm given by Hicks [7] using the Woods-Saxon single-nucleon wave functions, and falls very close to the middle between the two experimental values.

In Fig. 1, we plot the magnetic form factors of ^{17}O. In the figure, the solid curve shows the result of the pure contribution of the single $1d_{5/2}$ neutron; the dashed curve denotes the result including correction with $\alpha_1 = 0.887$, $\alpha_3 = 0.514$, and $\alpha_5 = 0.891$; the dotted curve represents the result including correction with α_1 fixed to $\mu_{\text{expt.}}/\mu_{s.n.} = 0.990$, $\alpha_3 = 0.475$, and $\alpha_5 = 0.880$, and the filled dots denote the experimental data from Refs. [1,7,17]. It is seen from Fig. 1 that the solid curve, i.e., the pure contribution of the single $1d_{5/2}$ neutron, gives a good approximate description for the shape of the experimental nuclear magnetic form factors, but the magnitude is noticeably larger within the momentum transfer region $q = (0.5\text{–}3.0)$ fm^{-1} than the experimental data and a little smaller in the high momentum region, $q > 3.0$ fm^{-1}. However, the contribution of the single $1d_{5/2}$ neutron is considerably brought down or modified after the quenching ratios are applied. The contribution of the single $1d_{5/2}$ neutron in the momentum transfer region $q = (0.5\text{–}2.5)$ fm^{-1} is properly quenched to agree well with the experimental data, and that in the momentum transfer region $q > 2.5$ fm^{-1} is slightly

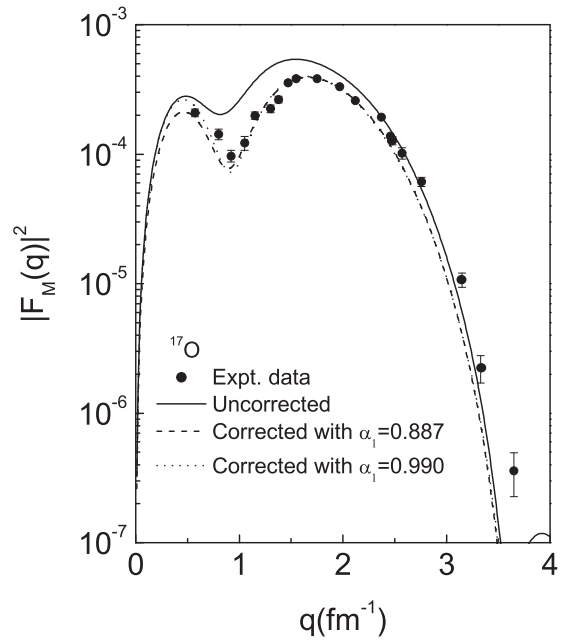

FIG. 1. The magnetic form factors of ^{17}O. The solid curve shows the result of the pure contribution of the single $1d_{5/2}$ neutron; the dashed curve denotes the result including correction with $\alpha_1 = 0.887$, $\alpha_3 = 0.514$, and $\alpha_5 = 0.891$; the dotted curve denotes that including correction with α_1 fixed to $\mu_{\text{expt.}}/\mu_{s.n.} = 0.990$, $\alpha_3 = 0.475$, and $\alpha_5 = 0.880$. The filled dots represent the experimental data from Refs. [1,7,17].

oversuppressed by the quenching ratios. The oversuppression of the single-nucleon contribution in the high momentum transfer region may be due to the underestimation of the magnetic form factors in this region within the relativistic mean field model. One possible reasonable explanation for the underestimation might be found in the calculations of ^{17}O using the natural orbitals obtained within the coherent density fluctuation model and containing nucleon correlation effects given by Kadrev *et al.* [28]. Their results of the magnetic form factors showed an important increase in the momentum transfer region $q = (1.5\text{–}3.5)$ fm^{-1}. Since the calculations contains no free parameters, the increase of the magnetic form factors should be an important result in theory.

Comparing the two sets of quenching ratios obtained in the present calculations, we can find that the values of α_5, 0.891 and 0.880, are nearly equal and close to unity. This may imply that the $M1$ and $M3$ multipoles do not contribute much to the magnetic form factors in the high momentum transfer region; i.e., the magnetic form factors in this region are dominated by the $M5$ multipole and can be described approximately by a single $1d_{5/2}$ neutron. The ratios $\alpha_3 = 0.514$ and 0.475 both indicate that the $M3$ multipole of the contribution of the single $1d_{5/2}$ neutron is significantly modified to agree with the experimental data. This may show that the meson exchange currents and core polarization effects could not be ignored and may bring considerable influence in the intermediate momentum transfer region for ^{17}O. This agrees with and supports the calculations given by Bohannon *et al.* [11], who first managed to calculate the core polarization effects by carrying out a Hartree-Fock calculation for the nucleus ^{17}O with a purely velocity-dependent Skyrme interaction plus a treatment of different deformations for the spin-up and spin-down nucleons. Their calculations led to a suppression of the $M3$ multipole of the form factors and as a result yielded the reduction of the magnetic form factors around $q = 1.0$ fm^{-1}.

We also note from Fig. 1 that either set of quenching ratios produces a good fit of the theoretical results to the available experimental data; however, the curve with the set of quenching ratios with $\alpha_1 = 0.887$ (dashed curve) and that with $\alpha_1 = 0.990$ (dotted curve) still have a small difference around $q = 0.5$ fm^{-1}. As a matter of fact, any value between 0.887 and 0.990 for α_1 can produce a good fit to the available experimental data. The appearance of the uncertainty of α_1 is due to lack of enough experimental data in the very low momentum transfer region. Nevertheless, the values of α_1 can still indicate that the $M1$ multipole is the dominant component of the magnetic form factors of ^{17}O in the low momentum transfer region and that it is to some extent reasonable to choose $\alpha_1 = \mu_{\text{expt.}}/\mu_{s.n.}$ for ^{17}O. However, we will see in the following discussions that such a way of setting the first multipole quenching ratio is not always valid.

In Fig. 2 we present the results of the nucleus ^{25}Mg. The solid curve denotes the result of the pure contribution of the single $1d_{5/2}$ neutron; the dashed curve shows the result including correction with the set of quenching ratios $\alpha_1 = 0.333$, $\alpha_3 = 0.205$, and $\alpha_5 = 0.510$, and the dotted curve indicates the result including correction with α_1 fixed to $\mu_{\text{expt.}}/\mu_{s.n.} = 0.447$, $\alpha_3 = 0.124$, and $\alpha_5 = 0.499$, where

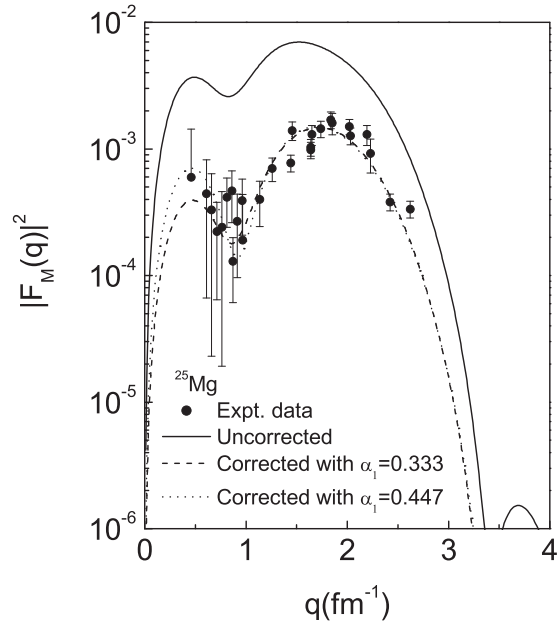

FIG. 2. The magnetic form factors of ^{25}Mg. The solid curve corresponds to the contribution of the single $1d_{5/2}$ neutron; the dashed curve corresponds to the result including correction with $\alpha_1 = 0.333$, $\alpha_3 = 0.205$, and $\alpha_5 = 0.510$, and the dotted curve corresponds to that including correction with $\alpha_1 = \mu_{\text{expt.}}/\mu_{s.n.} = 0.447$, $\alpha_3 = 0.124$, and $\alpha_5 = 0.499$. The filled dots represent the experimental data from Refs. [18,19].

$\mu_{\text{expt.}} = -0.85545\mu_N$ [55] for ^{25}Mg and $\mu_{s.n.} = -1.9130\mu_N$ for the neutron. The filled dots represent the experimental data from Refs. [18,19]. We can see from Fig. 2 that, similarly to ^{17}O, the contribution of the single $1d_{5/2}$ neutron also gives a close description of the shape of the experimental form factors, but the magnitude shows a considerable deviation from the experimental data, much larger than that of ^{17}O. This is mainly because ^{17}O has a doubly magic number core ^{16}O, while ^{25}Mg is a nucleus with the s-d shell nearly half filled, so its unpaired $1d_{5/2}$ orbital neutron may have a stronger coupling to the ^{24}Mg core. However, after the quenching ratios are applied, the contribution of the single $1d_{5/2}$ orbital neutron is brought down appropriately to produce a very good agreement with experiment. Although the results from the two sets of quenching ratios show conspicuous differences in the momentum transfer region $q = (0\text{–}1.5)$ fm $^{-1}$, the agreement of either calculated result with the experimental data is quite good, especially that with the set of quenching ratios with $\alpha_1 = \mu_{\text{expt.}}/\mu_{s.n.} = 0.447$. This again shows that it is, to a certain degree, reasonable to choose $\alpha_1 = \mu_{\text{expt.}}/\mu_{s.n.}$ for ^{25}Mg.

Our calculations of the magnetic form factors for ^{25}Mg agree with and support the results obtained by other authors. One very important theoretical result for the magnetic form factors of ^{25}Mg was obtained by Moya de Guerra and Dieperink [20] within the projected Hartree-Fock approximation using the Nilsson single-particle state functions. They carried out an investigation of the electromagnetic form factors of odd-A axially symmetric deformed nuclei within

the projected Hartree-Fock approximation and gave a general expression containing the important collective contributions of the core nucleons. The effectiveness of this method was well illustrated with specific calculations for ^{181}Ta and ^{25}Mg. The result for ^{25}Mg showed very good agreement with experimental data. They predicted a reduction of the $M3$ form factors by a factor 0.12 and a reduction of the $M5$ form factors by a factor 0.55 with respect to the single-nucleon contribution. The importance of the result obtained by Moya de Guerra and Dieperink lies in that their calculations for the reduction factors are parameter free and not fitted from the experimental data; both reduction factor values were obtained purely from the theory of collective rotational motion, and in this respect their calculations are superior to ours. Our results for the quenching ratios obtained with α_1 set to $\mu_{\text{expt.}}/\mu_{s.n.} = 0.447$ are very close to those obtained by these authors. In addition, more general and detailed theoretical studies and discussions on the calculations of nuclear form factors in the rotational model were also given by Moya de Guerra [21] in 1980. Another important result for ^{25}Mg was given by Euteneuer *et al.* [19]. They obtained two sets of quenching ratios for ^{25}Mg within a generalized single-particle model with the magnetic moment of ^{25}Mg fixed to its experimental value $-0.855\mu_N$. One set of the quenching ratios is $\alpha_1 = 0.455$, $\alpha_3 = 0.22 \pm 0.13$, and $\alpha_5 = 0.47 \pm 0.03$, which were obtained using the harmonic oscillator wave function with the harmonic oscillator length $b = 1.831$ fm, and the other set is $\alpha_1 = 0.455$, $\alpha_3 = 0.27 \pm 0.12$, and $\alpha_5 = 0.50 \pm 0.08$, which were obtained using the Woods-Saxon wave function with the skin thickness $a_0 = 0.65$ fm and the $1d$ shell separation energy fixed to -7.332 MeV. The two sets of quenching ratios obtained by these authors do not show much difference. For the set of quenching ratios that we obtained with α_1 fixed to $\mu_{\text{expt.}}/\mu_{s.n.} = 0.447$, the values $\alpha_1 = 0.447$ and $\alpha_5 = 0.499$ are very close to those given by these authors, but $\alpha_3 = 0.124$ is much smaller than those given by Euteneuer *et al.* For the other set of quenching ratios that we obtained with α_1 set free, the values of α_3 and α_5 are both close to those given by Euteneuer *et al.*, while the value $\alpha_1 = 0.333$ is a little smaller than that given the authors. However, the agreement of the present results with experimental data, especially that with $\alpha_1 = 0.447$, which appears to reveal the trend of variation of the form factors in the low momentum transfer region better, seems to be a little better near the minimum than that presented in Ref. [19]. In addition, compared with ^{17}O, the smaller quenching ratios for ^{25}Mg may imply that the many-body and core polarization effects could have stronger influences on the magnetization density distribution of ^{25}Mg.

^{27}Al is another s-d shell nucleus with a proton hole in the outermost $1d_{5/2}$ subshell. Among the considered nuclei, ^{27}Al is the only one whose measured magnetic moment is larger than that of the proton. Therefore, the calculation of ^{27}Al is of special interest, since the result will provide an opportunity to test if it is still valid to choose $\mu_{\text{expt.}}/\mu_{s.n.}$ as the first quenching ratio for this kind of nuclei in the case that the nuclear magnetic moment is greater than that of the valence nucleon. Figure 3 shows a comparison between the theoretical results and experimental data for ^{27}Al. In the figure, the solid curve denotes the result of the pure contribution of the single $1d_{5/2}$ proton; the dashed curve shows the result including correction with $\alpha_1 = 0.716$, $\alpha_3 = 0.435$, and $\alpha_5 = 0.606$, and the dotted curve shows the result including correction with α_1 fixed to $\mu_{\text{expt.}}/\mu_{s.n.} = 1.304$, $\alpha_3 = 1.90 \times 10^{-4}$, and $\alpha_5 = 0.575$, where $\mu_{\text{expt.}} = 3.6415\mu_N$ [55] for ^{27}Al and $\mu_{s.n.} = 2.7928\mu_N$ for the proton; the filled dots represent the experimental data from Refs. [1,23]. It can be found from Fig. 3 that the pure contribution of the single $1d_{5/2}$ proton gives a very close description of the shape of the experimental form factors, and a nearly perfect agreement of the calculated result with the available experimental data is obtained after the set of quenching ratios $\alpha_1 = 0.716$, $\alpha_3 = 0.435$, and $\alpha_5 = 0.606$ are applied. However, the other set of ratios with α_1 fixed to $\mu_{\text{expt.}}/\mu_{s.n.} = 1.304$ failed to reproduce the experimental data in the low and intermediate momentum transfer region $q = (0\text{–}2.5)$ fm^{-1}. This shows that choosing $\mu_{\text{expt.}}/\mu_{s.n.}$ as the value of the $M1$ multipole quenching ratio is no longer valid for ^{27}Al. This is in sharp contrast to the cases of ^{17}O, ^{25}Mg, ^{29}Si, and ^{31}P (^{29}Si and ^{31}P will be discussed in the following section). Nevertheless, we can still draw some useful information from the fitted values of α_5 and the results in the high momentum transfer region. The values of α_5 and the results in the high momentum transfer region may imply that for ^{27}Al the $M1$ and $M3$ multipoles of the contribution of the single $1d_{5/2}$ proton could not bring considerable effects in the high momentum transfer region $q \geqslant 2.5$ fm^{-1}, or in other words, the $M5$ multipole is mainly responsible in the high momentum transfer region.

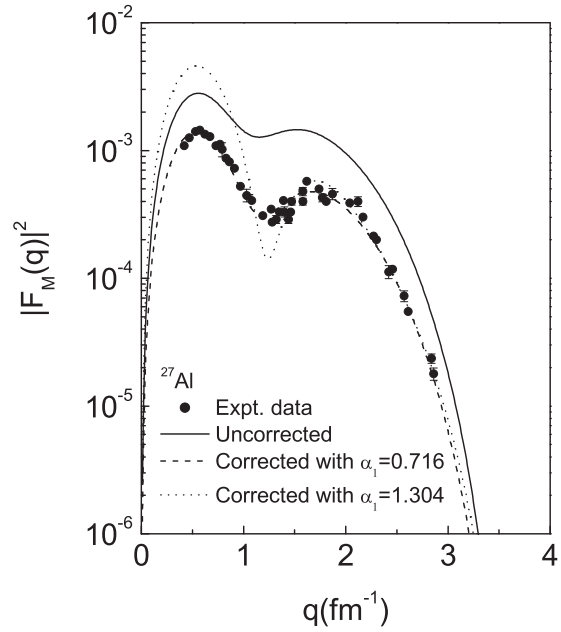

FIG. 3. The magnetic form factors of ^{27}Al. The solid curve corresponds to the contribution of the single $1d_{5/2}$ proton; the dashed curve corresponds to the result including correction with $\alpha_1 = 0.716$, $\alpha_3 = 0.435$, and $\alpha_5 = 0.606$, and the dotted curve corresponds to the result including correction with $\alpha_1 = \mu_{\text{expt.}}/\mu_{s.n.} = 1.304$, $\alpha_3 = 1.90 \times 10^{-4}$, and $\alpha_5 = 0.575$. The filled dots represent the experimental data from Refs. [1,23].

For ^{27}Al, direct theoretical calculations of the nuclear magnetic form factors containing modifications to the valence-nucleon contributions were also performed by some researchers. One good result was given in Ref. [1], which was obtained using the matrix elements of Brown and Wildenthal with the wave functions generated from the Woods-Saxon potential model with $r_0 = 1.12$ fm and $a = 0.72$ fm. Another calculation was carried out by Radhi *et al.* [29], who calculated the magnetic form factors of ^{17}O, ^{25}Mg, ^{27}Al in terms of the configuration mixing shell model plus core polarization effects with the nucleon wave functions from the harmonic oscillator potential model. They found that core polarization effects could improve calculations in the low and intermediate momentum transfer region, but the improvement was not large enough to give a good agreement with the experimental data. Their calculations also showed that, if the data in the high momentum transfer region were well described, the valence orbital had to be given a size smaller than that required by the rms charge radius.

B. The nuclei ^{31}P and ^{29}Si

In the s-d shell, ^{29}Si and ^{31}P are two typical spin-$\frac{1}{2}$ nuclei with a single nucleon in the outermost $2s_{1/2}$ orbital in the ground state, so they are of much interest for studying the form factors with contributions only from the $M1$ multipole. In the cases of ^{31}P and ^{29}Si, only the quenching ratio α_1 is needed. The quenching ratio will only shift the form factor curve up and down and will not change the shape. Therefore, ^{31}P and ^{29}Si may be good cases to explore how the shapes and intensities of the magnetization density distributions of the odd-A nuclei are influenced by the many-body and core polarization effects. In Table I, we have given the values of the quenching ratio α_1 for both nuclei, with one value fixed to $\mu_{\text{expt.}}/\mu_{s.n.}$ and the other fitted from the experimental data. In Figs. 4 and 5 we plot the results of the magnetic form factors for both nuclei. The solid curves correspond to the results of the contributions of the single $2s_{1/2}$ proton for ^{31}P and the single $2s_{1/2}$ neutron for ^{29}Si; the dashed curves show the results including correction with $\alpha_1 = 0.526$ for ^{31}P and $\alpha_1 = 0.532$ for ^{29}Si; the dotted curves show the results including correction with α_1 fixed to $\mu_{\text{expt.}}/\mu_{s.n.} = 0.405$ for ^{31}P and $\mu_{\text{expt.}}/\mu_{s.n.} = 0.290$ for ^{29}Si, where $\mu_{\text{expt.}} = 1.13160\mu_N$ [55] for ^{31}P and $\mu_{\text{expt.}} = -0.55529\mu_N$ [55] for ^{29}Si; the filled dots represent the experimental data from Refs. [1,22].

For ^{31}P, it is seen from Fig. 4 that the quenching ratio $\alpha_1 = 0.526$ reproduces very well the experimental data, except for a very slight discrepancy near $q = 1.5$ fm $^{-1}$, and that the ratio $\alpha_1 = \mu_{\text{expt.}}/\mu_{s.n.} = 0.405$ also reproduces well the experimental data, though the agreement is not as good as that given by $\alpha_1 = 0.526$. It is worth noting that the good agreement—the minimum and second maximum being accurately reproduced– is reached just by a simple shift down of the single $2s_{1/2}$ proton contribution. The shape of the experimental form factors are nearly exactly reproduced by the pure contribution of the single $2s_{1/2}$ proton. In view of the plane wave Born approximation, this implies that for ^{31}P the shape of the magnetization density distribution in radial space yielded by the motion of the single $2s_{1/2}$ proton could be very close to the actual situation, and the influences of the

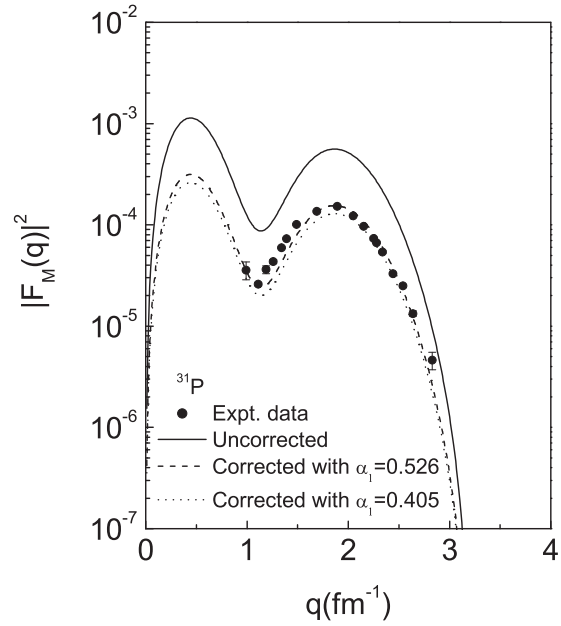

FIG. 4. The magnetic form factors of ^{31}P. The solid curve denotes the pure contribution of the single $2s_{1/2}$ proton; the dashed curve shows the result including correction with $\alpha_1 = 0.526$, and the dotted curve shows the result including correction with α_1 fixed to $\mu_{\text{expt.}}/\mu_{s.n.} = 0.405$. The filled dots represent the experimental data from Refs. [1,22].

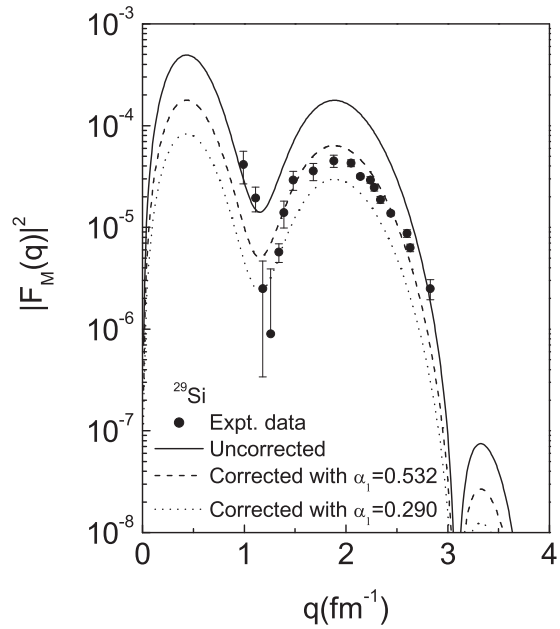

FIG. 5. The magnetic form factors of ^{29}Si. The solid curve corresponds to the pure contribution of the single $2s_{1/2}$ neutron; the dashed curve corresponds to the result including correction with $\alpha_1 = 0.532$, and the dotted curve corresponds to the result including correction with $\alpha_1 = \mu_{\text{expt.}}/\mu_{s.n.} = 0.290$. The filled dots show the experimental data from Refs. [1,22].

many-body and core polarization effects should be mainly on the intensities of the magnetization distribution.

For ^{29}Si, the agreements between the experimental data and the calculations with the two sets of quenching ratios, $\alpha_1 = 0.532$ and $\alpha_1 = \mu_{\text{expt.}}/\mu_{s.n.} = 0.290$, are neither as good as that of ^{31}P. The result given by $\alpha_1 = 0.532$ shows an obvious deviation from the experimental data in the momentum transfer region around $q = 1.0$ fm $^{-1}$, and the result given by $\alpha_1 = \mu_{\text{exp}}/\mu_{sn} = 0.290$ shows a larger deviation from the experimental data nearly over the whole momentum transfer range except at the minimum. This indicates that for ^{29}Si both the shape and intensities of the radial magnetization density distribution yielded by the motion of the single $2s_{1/2}$ neutron have deviations from the actual situation of ^{29}Si. This may show that, unlike ^{31}P, the many-body and core polarization effects could play an important role in determining both the shape and the intensities of the magnetization density distribution of ^{29}Si.

As for calculations of the magnetic form factors of ^{29}Si and ^{31}P, direct theoretical calculations were also carried out by some authors. Here, we would like to specially mention the work of Graca *et al.* [8]. Unlike most calculations in the spherical models, these authors considered ^{29}Si in the deformed model. Using the Nilsson wave functions they built a connection between the deformation parameter and the nuclear magnetic form factors. Their calculations of ^{29}Si are in good agreement with experimental data. In their calculations, the quenching or reduction of the magnetic form factors with respect to the single nucleon contribution comes out as a natural result of the theory on nuclear collective motion. A more general analysis was also given by these authors, which showed that this method could be applicable to many odd-nucleon Nilsson orbital nuclei.

Now we are on the point of finishing the discussions of the results of ^{17}O, ^{25}Mg, ^{27}Al, ^{29}Si, and ^{31}P. However, before we come to an end, a few remarks should be made on the method and results of the present research. We investigated the magnetic form factors of ^{17}O, ^{25}Mg, ^{27}Al, ^{29}Si, and ^{31}P within the relativistic frame with the single nucleon wave functions generated by the relativistic mean field model, and obtained two sets of quenching ratios for the nuclear magnetic form factors for each nucleus and discussed the physical implications. The results, on the one hand, show that very good fits to the experimental magnetic form factors of the considered nuclei can be obtained using the single valence-nucleon wave functions from the relativistic mean field model. This may show that the wave functions given by the relativistic mean field model are reliable and can give a fairly accurate description for the motion of the nucleons in nuclei. However, on the other hand, the results may also show that the shapes and intensities of the magnetization distributions yielded by the single valence-nucleon wave functions, in particular the intensities, are just an approximation to the real nuclear magnetization distributions. The deviation is mainly due to two reasons: one is the many-body effects, such as those of the meson exchange and back-flow currents in the relativistic mean field, and the other is the core polarization effect. Apart from the two main reasons, there may be a configuration admixtures effect for ^{25}Mg, ^{27}Al, ^{29}Si, and ^{31}P and a deformation effect for ^{25}Mg. All these effects are just considered by phenomenologically introducing the quenching ratios in the present research. This method may be applied nearly to all the odd-A nuclei, and enables us to avoid being brought into complicated mathematical calculations and get a general idea that to what degree elastic magnetic electron scattering off odd-A nuclei can be described by the single valence nucleon. However, if we want to understand more about the physics behind the quenching ratios, to grasp the physical meaning, direct theoretical calculations containing the many-body effects and/or the core polarization effects with reasonable methods on the microscopic level must be carried out.

As a matter of fact, many authors have made useful explorations from various different considerations of the many-body and core polarization effects to explain the deviations between the single valence-nucleon contributions and the observed nuclear magnetic form factors, and have acquired important and instructive results, such as those [1,8,11,19–21,28,29] that we have mentioned in the previous paragraphs. However, the overall situation is that the theoretical explanations of experiments in this respect are still not very satisfactory, and further research work is still needed. As the quenching ratios have shown, the deviations between the single valence-nucleon contributions and the experimental data differ very much for different nuclei; the many-body and core polarization effects may need to be treated differently for each nucleus. This might be the key point in dealing with the many-body and core polarization effects. To find targeted and workable forms of modification for a specific nucleus, perhaps the quenching ratios could provide references for estimating how strong the many-body and core polarization effects are in a specific nucleus, on which multipole(s) these effects mainly bring influence, and whether these effects bring changes to the positions of the minima and maxima predicted by the single valence nucleon. Perhaps these considerations along with the available calculations may be beneficial to further studies. We will try to consider incorporating the meson exchange currents and/or core polarization effects in calculating the magnetic form factors based on the relativistic mean field model in our following research work and expect that some new results could be obtained.

One more point that we would like to remark upon concerns the calculations of the form factors using nuclear models with free parameters such as the the harmonic oscillator potential model and the Woods-Saxon potential model. The harmonic oscillator potential model and the Woods-Saxon potential model are two of the most frequently used models in nuclear physics. In general, when the harmonic oscillator potential model is used to calculate the nuclear properties, the value of the harmonic-oscillator length b is usually assigned to satisfy the requirement of the rms radius of nuclear charge density distribution. For simplicity, in most cases, we choose $b = 1.0A^{1/6}$ fm or $b = 6.44(45A^{-1/3} - 25A^{-2/3})^{-1/2}$ fm [56] to approximately meet this requirement. However, it is not always necessary to do so; it might be more beneficial to take b as a free parameter in certain cases. In view of the

plane wave Born approximation, the shape of the magnetic form factors of an odd-A nucleus is dictated by the Bessel functions and the rms radius of the unpaired valence-nucleon wave function; so, in principle, a satisfactory shape for the magnetic form factors could be obtained in the harmonic oscillator model by adjusting the free parameter b to enable the unpaired valence-nucleon wave function to have a proper rms radius. Therefore, If we take b as a free parameter in calculating the magnetic form factors of nuclei, we could take better advantage of the model, although in this case we may to a certain extent sacrifice the compatibility between b and the rms radius of charge density distribution. Taking b as a free parameter may allow the results given within the other models to be easily repeated in the harmonic oscillator model and compared and discussed, and, moreover, this may provide a way to explore to what extent the shape of the nuclear magnetic form factors may be noticeably affected by the varying shapes of the unpaired valence-nucleon wave function. To perform this, the calculated rms radii of the corresponding single valence wave functions listed in Table I, for instance, can be used as references for calculations of the magnetic form factors in the harmonic oscillator potential model. We could adjust b to enable the corresponding single valence-nucleon wave functions to have the same rms radii as those listed in Table I and calculate the magnetic form factors and the corresponding single valence-nucleon wave functions. Then the results of the magnetic form factors and the corresponding single valence-nucleon wave functions from the harmonic oscillator model and RMF model could be compared and discussed. In this way, perhaps we could get information about the role played by the shape of the valence nucleon wave function in determining the nuclear magnetic form factors of the odd-A nuclei.

IV. SUMMARY

The magnetic form factors of the *s-d* shell odd-A nuclei ^{17}O, ^{25}Mg, ^{27}Al, ^{29}Si, and ^{31}P are investigated within the relativistic frame with single-nucleon wave functions generated using the relativistic mean field model. The single valence-nucleon contributions to the nuclear magnetic form factors are calculated, and two sets of quenching ratios of the magnetic form factors relative to the single valence-nucleon contribution are extracted for each nucleus. It is found that the single valence-nucleon contributions can give a good approximate description of the shapes of the nuclear form factors, including the positions of the minima and maxima. With the quenching ratios obtained with α_1 set free, the experimental magnetic form factors of the considered nuclei can be reproduced quite well. With the quenching ratios obtained with α_1 fixed to $\mu_{\text{expt.}}/\mu_{s.n.}$, situations appear to vary: for ^{17}O, ^{25}Mg, ^{29}Si, and ^{31}P, the experimental data can be well or very satisfactorily reproduced, but for ^{27}Al the experimental form factors could not be reproduced in the low and medium region. This shows that choosing $\mu_{\text{expt.}}/\mu_{s.n.}$ as the $M1$ multipole quenching ratio makes sense only to part of the odd-A nuclei, perhaps a large part. In addition, the successful reproduction of the experimental data of ^{17}O, ^{25}Mg, ^{27}Al, ^{29}Si, and ^{31}P using the relativistic mean field model just by introducing the quenching ratios indicates that the single nucleon wave functions generated by the relativistic mean field model are reliable. Moreover, the present calculations have no adjustable parameters for specific nuclei, and could be a good complement from the relativistic frame to the available results obtained within the other nuclear models and provide more useful references for further and more involved studies.

ACKNOWLEDGMENTS

This work is supported by the National Natural Science Foundation of China (Grants No. 11275138, No. 11375086, No. 10675090, and No.11404241), by the Scientific and Technological development Project of Tianjin Educational Committee (Grant No .20100911), and by the Research Fund of Tianjin University of Technology and Education (Grant No. KJYB11-3).

[1] T. W. Donnelly and I. Sick, Rev. Mod. Phys. **56**, 461 (1984).
[2] R. Hofstadter, Rev. Mod. Phys. **28**, 214 (1956).
[3] R. Hofstadter, Annu. Rev. Nucl. Sci. **7**, 231 (1957).
[4] R. Hofstadter, *Nodel Lecture 1961*, Nobel Lectures – Physics (Elsevier, Amsterdam, 1964).
[5] H. Überall, *Electron Scattering from Complex Nuclei* (Academic Press, New York, 1971).
[6] J. Heisenberg and H. P. Blok, Annu. Rev. Nucl. Part. Sci. **33**, 569 (1983).
[7] R. S. Hicks, Phys. Rev. C **25**, 695 (1982).
[8] E. Graca, P. Sarriguren, D. Berdichevsky *et al.*, Nucl. Phys. A **483**, 77 (1988).
[9] E. Moya de Guerra and S. Kowalski, Phys. Rev. C **20**, 357 (1979).
[10] E. Moya de Guerra and S. Kowalski, Phys. Rev. C **22**, 1308 (1980).
[11] G. Bohannon, L. Zamick, and E. Moya de Guerra, Nucl. Phys. A **334**, 278 (1980).
[12] P. Sarriguren, E. Moya de Guerra, R. Nojarov, and A. Faessler, J. Phys. G **20**, 315 (1994).
[13] J. D. Walecka, *Electron Scattering for Nuclear and Nucleon Structure* (Cambridge University Press, Cambridge, 2001).
[14] J. Karataglidis and K. Amos, Phys. Lett. B **650**, 148 (2007).
[15] H. Baghaei *et al.*, Phys. Rev. C **42**, 2358 (1990).
[16] M. V. Hynes *et al.*, Phys. Rev. Lett. **42**, 1444 (1979).
[17] N. Kalantar-Nayestanaki, H. Baghaei, W. Bertozzi *et al.*, Phys. Rev. Lett. **60**, 1707 (1988).
[18] R. C. York and G. A. Peterson, Phys. Rev. C **19**, 574 (1979).
[19] H. Euteneuer, H. Rothhaas, O. Schwentker *et al.*, Phys. Rev. C **16**, 1703 (1977).
[20] E. Moya de Guerra and A. E. L. Dieperink, Phys. Rev. C **18**, 1596 (1978).

[21] E. Moya de Guerra, Ann. Phys. (N.Y.) **128**, 286 (1980).
[22] H. Miessen, H. Rothhaas, G. Lührs, G. A. Peterson *et al.*, Nucl. Phys. A **430**, 189 (1984).
[23] L. Lapikas, A. E. L. Dieperink, and G. Box, Nucl. Phys. A **203**, 609 (1973).
[24] S. Platchkov *et al.*, Phys. Rev. Lett. **61**, 1465 (1988).
[25] E. Garrido and E. Moya de Guerra, Nucl. Phys. A **650**, 387 (1999); Phys. Lett. B **488**, 68 (2000).
[26] A. N. Antonov, D. N. Kadrev, M. K. Gaidarov, E. Moya de Guerra, P. Sarriguren, J. M. Udías, V. K. Lukyanov, E. V. Zemlyanaya, and G. Z. Krumova, Phys. Rev. C **72**, 044307 (2005).
[27] P. Sarriguren, M. K. Gaidarov, E. M. de Guerra, and A. N. Antonov, Phys. Rev. C **76**, 044322 (2007).
[28] D. N. Kadrev, A. N. Antonov, M. V. Stoitsov, and S. S. Dimitrova, Int. J. Mod. Phys. E **5**, 717 (1996).
[29] R. A. Radhi, N. T. Khalaf, and A. A. Najim, Nucl. Phys. A **724**, 333 (2003).
[30] J. D. Walecka, Ann. Phys. (N.Y.) **83**, 491 (1974).
[31] J. D. Walecka, Phys. Lett. B **94**, 293 (1980).
[32] B. D. Serot and J. D. Walecka, in *Advances in Nuclear Physics*, edited by J. W. Negele and E. Vogt, Vol. 16 (Plenum, New York, 1986).
[33] C. J. Horowitz and B. D. Serot, Nucl. Phys. A **368**, 503 (1981).
[34] Y. K. Gambhir, P. Ring, and A. Thimet, Ann. Phys. (N.Y.) **198**, 132 (1990).
[35] M. M. Sharma, M. A. Nagarajan, and P. Ring, Phys. Lett. B **312**, 377 (1993).
[36] Z. Ma, H. Shi, and B. Chen, Phys. Rev. C **50**, 3170 (1994).
[37] G. A. Lalazissis, J. König, and P. Ring, Phys. Rev. C **55**, 540 (1997).
[38] Z. Ren, W. Mittig, and F. Sarazin, Nucl. Phys. A **652**, 250 (1999).
[39] Z. Ren, W. Mittig, B. Chen, and Z. Ma, Phys. Rev. C **52**, R20 (1995).
[40] Y. Sugahara and H. Toki, Nucl. Phys. A **579**, 557 (1994).
[41] B. G. Todd-Rutel and J. Piekarewicz, Phys. Rev. Lett. **95**, 122501 (2005).
[42] J. E. Amaro, J. A. Caballero, T. W. Donnelly, and E. Moya de Guerra, Nucl. Phys. A **611**, 163 (1996).
[43] J. A. Caballero, T. W. Donnelly, E. Moya de Guerra, and J. M. Udías, Nucl. Phys. A **632**, 323 (1998).
[44] J. A. Caballero, T. W. Donnelly, E. Moya de Guerra, and J. M. Udías, Nucl. Phys. A **643**, 189 (1998).
[45] J. M. Udías, P. Sarriguren, E. Moya de Guerra, E. Garrido, and J. A. Caballero, Phys. Rev. C **48**, 2731 (1993); **51**, 3246 (1995).
[46] Y. Jin, D. S. Onley, and L. E. Wright, Phys. Rev. C **45**, 1311 (1992).
[47] J. D. Bjorken and S. D. Drell, *Relativistic Quantum Mechanics* (McGraw-Hill, New York, 1964).
[48] T. de Forest and J. D. Walecka, Adv. Phys. **15**, 1 (1966).
[49] T. W. Donnelly and J. D. Walecka, Nucl. Phys. A **201**, 81 (1973).
[50] A. R. Edmonds, *Angular Momentum in Quantum Mechanics* (Princeton University Press, Princeton, New Jersey, 1960).
[51] E. J. Kim, Phys. Lett. B **174**, 233 (1986).
[52] B. D. Serot, Phys. Lett. B **107**, 263 (1981).
[53] R. S. Willey, Nucl. Phys. **40**, 529 (1963).
[54] H. de Vries, C. W. de Jager, and C. de Vries, At. Data Nucl. Data Tables **36**, 495 (1987).
[55] P. Raghavan, At. Data Nucl. Data Tables **42**, 189 (1989).
[56] J. Blomqvist and A. Molinari, Nucl. Phys. A **106**, 545 (1968).